Multipoint Bending Measurement Using Multicore Fiber Bragg Grating and Two-Photon Absorption Process in Si-APD

Naohiro Sonoda, Reina Takagi, Itsuki Saito, Tetsuya Abe, Shihua Zhao, and Yosuke Tanaka, *Member, IEEE*

***Abstract*—We propose and demonstrate a fiber optic multi-point bending measurement system that uses Bragg gratings inscribed along a multi-core fiber (MCF) and a silicon avalanche photodiode (Si-APD) that produces two-photon absorption (TPA) photocurrent for 1.55-μm light. Because the TPA photocurrent from the Si-APD is proportional to the mean square of the optical intensity, the intensity correlation between 1.55-μm probe and reference beams is measured from it without using complex electrical circuits. The proposed system has different lengths of optical fibers between each core of MCF and input/output ends of a single mode fiber optic system, which makes different the correlation signal between the reference beam and the probe beam reflected from different Bragg gratings in MCF. That enables the reflection spectra of all the Bragg gratings in MCF to be separately measured even when they are overlapped in the wavelength domain. As a result, the bending radius and its direction are measured without using multiple detectors or optical switching devices. We conducted proof-of-concept experiments by using a 7-core MCF with almost the same Bragg gratings inscribed in each core at three points along the fiber. We also demonstrated an example of application to shape measurement.**

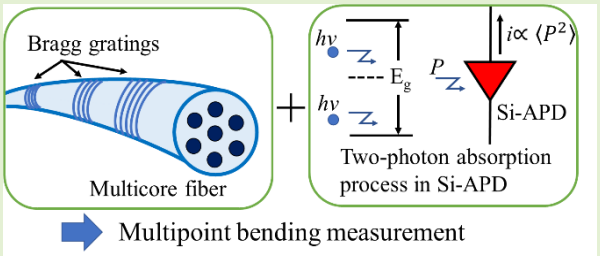

***Index Terms*— Bending measurement, fiber Bragg grating, multicore fiber, optical fiber sensor, two-photon absorption process.**

I. Introduction

BENDING measurement is an important technology that is required in applications such as shape measurement and health monitoring of structures. Among various methods having been developed, optical fiber-based bending sensors have attractive features of non-invasiveness to the human body, electromagnetic-noise-free operation, and mechanically flexible properties. Because of these characteristics, the fiber optic bending sensors are expected to be applied to bending measurement of medical instruments, robot arms, and structural health monitoring for bridges, tunnels, and aircrafts. The typical fiber optic bending sensors include (i) modulation-based ones that change their output optical power according to the bend-induced transmission loss [1]–[3] and (ii) Bragg-grating- or long-period-grating-based ones that change their Bragg wavelengths or resonance wavelengths by the applied bending [4]–[6]. The bending sensor based on Brillouin frequency shift in an optical fiber [7], [8], Rayleigh backscattering [9], and Fabry-Perot interferometer [10] are also proposed. A sophisticated system using Rayleigh backscattering has achieved distributed sensing with a high spatial resolution and successfully measured a needle shape [9]. The Fabry-Perot method is especially useful for measuring small curvature at a single point [10]. In principle, a bending sensor using a single fiber with a single core measures in-plane bending. Three-dimensional bending measurement needs multiple waveguides. Some methods use multiple optical fibers with Bragg gratings for this purpose [11]. The grating-based methods are employed easily without using complex signal processing and useful for shape measurement with a relatively lower spatial resolution. Some other recently proposed methods use a multicore fiber with Bragg gratings (MCFBG) inscribed in each core [12], which realize three-dimensional bending measurement with one optical fiber [13]–[17]. In the MCFBG-based bending measurement, we need to discriminate reflection spectra of different Bragg gratings. If the Bragg wavelengths are sufficiently separated, the reflection spectra

Manuscript received August 16, 2021; revised October 1, 2021; accepted October 1, 2021. Date of publication October 4, 2021; date of current version November 12, 2021. This work was supported by JSPS KAKENHI Grant Number JP20H02158. The associate editor coordinating the review of this article and approving it for publication was Prof. Arnaldo G. Leal-Junior. *(Corresponding author: Yosuke Tanaka.)*

The authors are with the Department of Electrical and Electronic Engineering, Graduate School of Engineering, Tokyo University of Agriculture and Technology, Tokyo 184-8588, Japan (e-mail: s204389u@st.go.tuat.ac.jp; tyosuke@cc.tuat.ac.jp).

Digital Object Identifier 10.1109/JSEN.2021.3117858

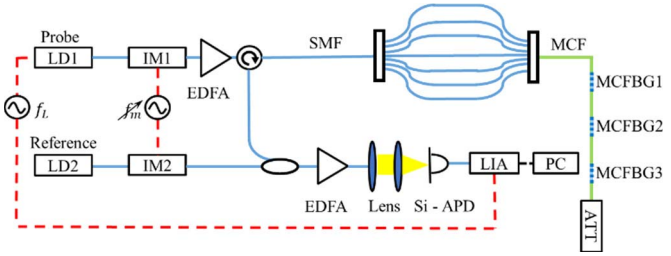

Fig. 1. Experimental setup for multipoint bending measurement system using multicore fiber Bragg gratings and two-photon absorption process in Si-APD. Red dashed line is electrical connections, blue solid line is single mode fiber (SMF), and green solid line is multicore fiber (MCF).

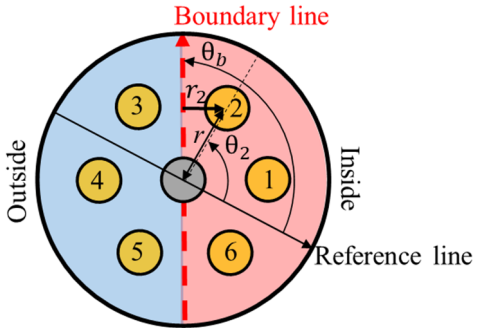

Fig. 2. Cross section of MCFBG.

and their shift can be easily identified [14]. However, sophisticated techniques are required to inscribe different Bragg gratings in the neighboring cores. On the other hand, MCFBG with the same grating in the neighboring cores is relatively easier to fabricate. However, bending sensors using such an MCFBG generally need to change the optical path or use multiple detectors to identify the reflected optical signal from the different cores [15], [16], which makes the system complex.

In this paper, we propose a fiber optic multi-point bending measurement system that uses MCFBGs having almost the same Bragg wavelength and a silicon avalanche photodiode (Si-APD) that produces two-photon absorption (TPA) photocurrent. The proposed method is based on intensity correlation measurement using TPA process in a Si-APD, which does not require multiple light sources, detectors, nor optical switching devices [18], [19]. In the last study, we have qualitatively performed the proof-of-concept experiment with a single point sensing part [20]. In this study, we investigate multipoint bending measurement. In addition, we will demonstrate an example of application to shape measurement.

II. Principle

A. Measurement of Reflection Spectra Using TPA Photocurrent of Si-APD

Fig.1 shows an experimental setup for multipoint bending measurement using MCFBG and TPA process in a Si-APD. Two laser diodes at 1.55 μm, LD1 and LD2, are used to produce probe and reference beams, respectively. The reference beam is modulated by the frequency f_m. The probe beam is firstly modulated by the frequency f_L for synchronous detection and then it is modulated by the frequency f_m. Then the probe beam is split by a splitter and each beam is injected into each core of a MCF through a fan-in device. These beams are reflected by the multiple gratings inscribed in the MCF and pass through an optical circulator to be combined with the reference beam. Finally, it is focused on a Si-APD and the intensity-correlation signal from it is obtained through a lock-in amplifier (LIA).

Although the Si-APD is usually insensitive to the light in the 1.55 μm wavelength band, high intensity light can induce the TPA process to produce photocurrent in proportion to the mean square of the light intensity. Using the square characteristic of TPA photocurrent, the intensity correlation between the probe signal and the reference light is measured without using expensive and complicated electronic circuits. The intensity correlation signal obtained by LIA is [18], [19]

$$i_{LIA} = const + \beta \sum_{j=1}^{N} I_{p,j} \cos\left(2\pi f_m \frac{n\Delta L_j}{c}\right), \tag{1}$$

where β is the proportional constant, $I_{p,j}$ is the intensity of the probe beam reflected by the j-th Bragg grating, n is the refractive index of the fiber, ΔL_j is the difference in transmission length between the probe beam reflected by the j-th Bragg grating and the reference beam, and c is the speed of light. Eq. (1) shows that sweeping the modulation frequency f_m induces periodical change of the cosine components in the intensity correlation signal, where the period of the cosine component with ΔL_j is

$$f_j = \frac{c}{n\Delta L_j}, \tag{2}$$

which is inversely proportional to ΔL_j. This means that Fourier peaks of the intensity correlation signal gives ΔL_j. In the proposed system, ΔL_j is set different by inserting different lengths of optical fibers between the splitter and the fan-in device. Here, the amplitude of Fourier peaks are proportional to $I_{p,j}$, which is proportional to the Bragg grating's reflectance for the wavelength of the probe beam. Under these conditions, even if the reflection spectra of the Bragg gratings overlap in the wavelength domain, we can separately measure them by using the Fourier spectra of the intensity correlation signals obtained for the different wavelengths of probe light.

B. Measurement of Curvature and Bending Direction

In a relatively narrow wavelength range of 10 nm or less, the Bragg wavelength of a fiber grating is supposed to be changed linearly with strain and temperature as

$$\lambda_B = S\Delta\varepsilon + K\Delta T, \tag{3}$$

where S is the strain coefficient, $\Delta\varepsilon$ is the strain change, K is the temperature coefficient, and ΔT is the temperature change.

Fig.2 shows a cross section of MCFBG used in this study, which consists of one central core and equally spacing six outer cores. The solid line that connects the midpoint of cores 1 and 6 and that of cores 3 and 4 is the reference line.

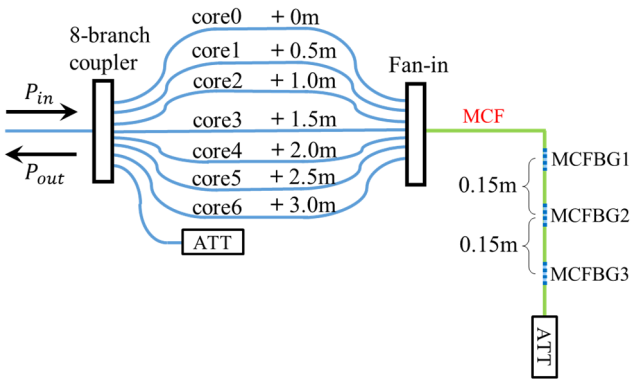

Fig. 3. Optical path length design of multicore FBG bending measurement system.

The dashed line is the boundary that separates the inner and outer regions of the bend. Let the angle of the boundary line against the reference one be θ_b and the angle of the line connecting the j-th outer and the central cores against the reference line be θ_j. The strain applied to the grating in the j-th outer core is expressed as follows [8], [9].

$$\varepsilon_j = \frac{r_j}{R} + \epsilon_{j0} = \kappa r sin\left(\theta_j - \theta_b\right) + \epsilon_0, \tag{4}$$

where r_j is the distance from the boundary line to the j-th outer core, κ is the curvature (reciprocal of the curvature radius R), r is the distance of the outer core from the central one, which is the same as the core pitch in the seven-core MCF, and ϵ_{j0} is the initial strain before bending, which is the same as the tensile strain applied to the central core. Note that because of the symmetric structure, the Bragg wavelength of the grating in the central core is basically independent of bending. Supposing that the temperatures of all cores are the same, the bending-induced Bragg wavelength shift of the grating in the j-th core is

$$\Delta\lambda_{jB} = S\left(\varepsilon_j - \varepsilon_0\right), \tag{5}$$

where S is the strain coefficient. Using Eqs. (4) and (5), we can derive the curvature radius R and the bending direction θ_b.

III. Experimental Setup

A. Design of Multipoint MCFBG System

We conducted experiments using a 7-core MCF with Bragg gratings inscribed at three points (MCFBG 1, 2, 3) along the fiber, which consists of 21 Bragg gratings in total. In our method, the path lengths of the probe beams reflected at different gratings have to be different from each other so that we can separately measure the reflection spectra. In this experiment, the distance between the neighboring MCFBG was set at 0.15 m. In addition, fibers with lengths of 0.5, 1.0, . . . , 3.0 m were inserted between the splitter and the fan-in device (Fig. 3). Table I shows the optical path length difference of the probe beams reflected once at MCFBG N ($N = 1, 2, 3$) in core j ($j = 0, 1, 2, \ldots, 6$) from that reflected at MCFBG 1 in the core0, which we call relative propagation length hereafter. Because all the optical path length differences

TABLE I
Optical Path Length Difference of Probe Beam Reflected Once at MCFBG N ($N = 1, 2, 3$) in Core j ($j = 0, 1, 2, \ldots, 6$) From the Beam Reflected at MCFBG 1 in Core0

	Core0	Core1	Core2	Core3	Core4	Core5	Core6
MCFBG1	0m	1.5m	3.0m	4.5m	6.0m	7.5m	9.0m
MCFBG2	0.45m	1.95m	3.45m	4.95m	6.45m	7.95m	9.45m
MCFBG3	0.9m	2.4m	3.9m	5.4m	6.9m	8.4m	9.9m

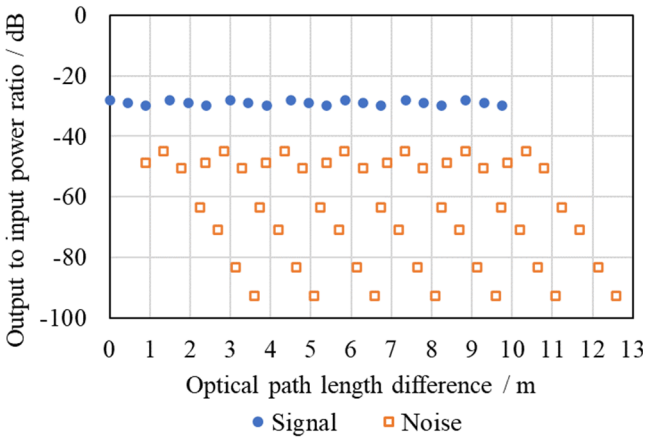

Fig. 4. Output to input power ratio of probe and noise component.

are different from each other, the reflection spectra can be separately observed.

The probe beam passes back and forth through an 8-branch optical splitter, which attenuates the optical power down to less than 1/64. Some part of the probe beam is reflected by the Bragg gratings multiple times and its propagation path length can be the same as the beam reflected only once at one of the Bragg gratings, which makes noise. The powers of such noise beams were calculated, assuming the same reflectance for all the gratings and a maximum reflection number of 7 times. In this calculation, we found that the reflectance of 10% is approximately the optimum value to minimize the noise power. Fig. 4 shows the simulated output to input power ratio of the probe beam reflected once at a Bragg grating and the noise component generated by the multiple reflection as a function of relative propagation length, where the reflectance of the gratings is assumed to be 10%. The probe signal appears at the relative propagation length of $1.5k$, $0.45{+}1.5k$, $0.9{+}1.5k$ [m], while the noise component appears at $0.9{+}1.5k$, $1.35{+}1.5k$, $1.8{+}1.5k$ [m] ($k = 0, 1, 2\ldots$). The signal to noise ratio of more than 10 dB is guaranteed.

IV. Experimental Results

A. Bending Measurement Using Multipoint MCFBG

In the experiment, the modulation frequency of probe and reference was swept over 2 GHz with a step of 2.5 MHz, which gives a spatial resolution of 0.15 m [19]. First, the sensing fiber was wound with a radius of 3 cm. Fig.5 shows the Fourier spectrum of the obtained signal as a function of the optical path length difference between the probe light reflected at

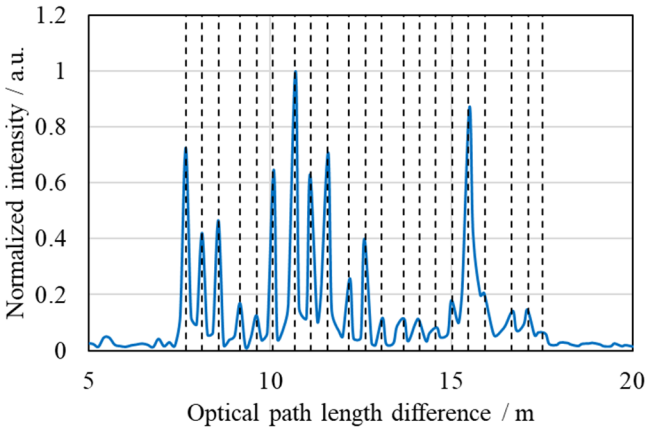

Fig. 5. Reflection points of MCFBG.

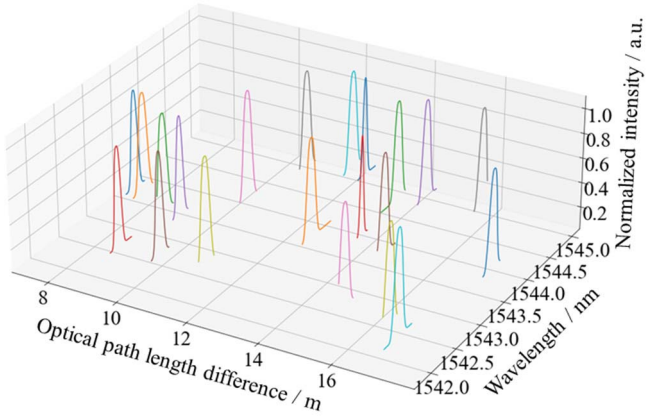

Fig. 6. Measured reflection spectra of all the Bragg gratings.

each reflection point of MCFBG and the reference light. The spectrum has 21 peaks corresponding to the number of Bragg gratings.

The reflection spectra of all the gratings were obtained by (i) sweeping the wavelength of the probe beam with a step of 0.04 nm, (ii) deriving the Fourier spectrum for each probe wavelength, and (iii) curve fitting the peaks of the Fourier spectra in the wavelength domain. Fig.6 shows the obtained reflection spectra of all the gratings, where the data points were fit by super Gaussian function. Fig.7 shows the bend-induced wavelength shift of the outer core Bragg gratings as a function of the outer core number, which is derived by subtracting the Bragg wavelength of the center core grating from that of the outer one. The influence of the temperature change and the initial tensile strain is canceled by the subtraction. In fact, temperature and tensile strain equally shift the Bragg wavelengths of the gratings in the neighboring cores. In addition, Bragg wavelength is not changed by the bending in the center core grating, because the effect of bend-induced compression and expansion of the grating pitch around the neutral axis is cancelled out. From Eqs. (4) and (5) with the fact that the outer cores are equally spaced, the data of Bragg wavelength shifts are fit with a sinusoidal function in principle, where the amplitude and the phase of the sinusoidal function correspond to the curvature and the bending direction, respectively. The amplitudes of all the sinusoidal curves A_w

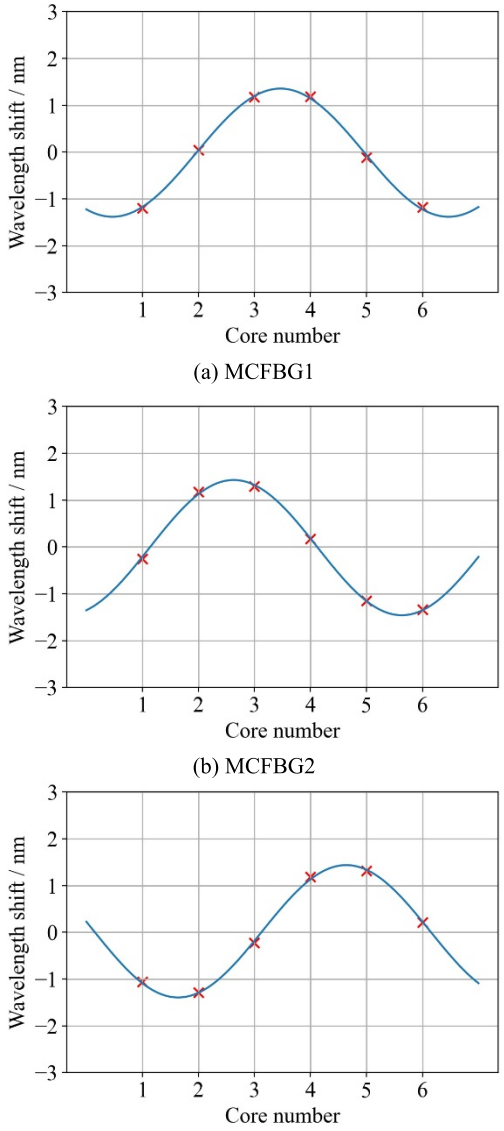

Fig. 7. Bend-induced wavelength shift of the outer core Bragg gratings as a function of the outer core number for MCFBG1, 2, 3 in Fig. 3, where the multicore fiber is wound with a curvature radius of 3 cm.

are the same, which corresponds to the experimental condition. A slight difference in phase is due to the twisting of the fiber.

B. Evaluation of Measurement on Bend-Induced Bragg Wavelength Shift and Bending Direction

First, we bent MCFBGs in a plane with the same curvature (the reciprocal of bending radius) κ of 0.100 to 0.333 cm^{-1} at the same time and obtained the sinusoidal curves for each curvature in the same manner as Fig.7. The amplitude A_w of the sinusoidal curve was measured for each curvature from the mean value of five times measurements. Fig.8 shows that A_w linearly changes with the curvature. Note that the least square lines do not pass through the original point, which is thought to be due to the ununiform strain of the fiber. We calculated the slope $dA_w/d\kappa$, which is the sensitivity to bend, and its standard deviation (Table II). Here, the theoretical value of

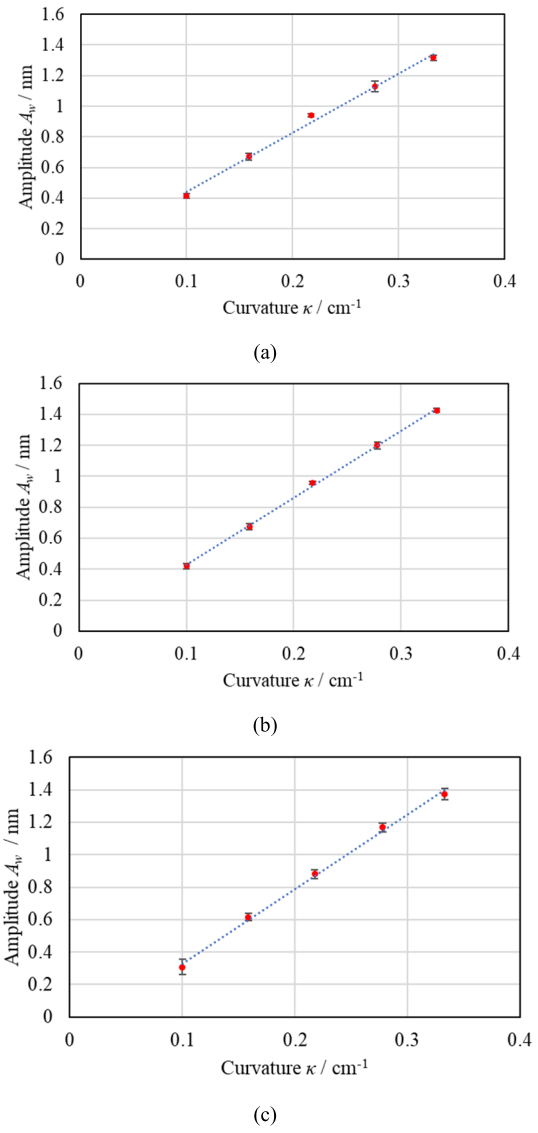

Fig. 8. Amplitude of sinusoidal curve obtained as a function of outer core number A_W vs. set curvature κ for (a) MCFBG1, (b) MCFBG2, and (c) MCFBG3.

TABLE II
THE SLOPE OF BEND-INDUCED WAVELENGTH SHIFT AS A FUNCTION OF CURVATURE AND THE STANDARD DEVIATION OF WAVELENGTH SHIFT

	Slope [nm / cm^{-1}]	Standard deviation [nm]				
		κ = 0.100 cm^{-1}	κ = 0.159 cm^{-1}	κ = 0.217 cm^{-1}	κ = 0.278 cm^{-1}	κ = 0.333 cm^{-1}
MCFBG1	3.87	0.0138	0.0232	0.0112	0.0364	0.0191
MCFBG2	4.33	0.0175	0.0208	0.0105	0.0224	0.0134
MCFBG3	4.59	0.0473	0.0221	0.0269	0.0267	0.0354

the slope is

$$\frac{dA_w}{d\kappa} = \frac{dA_w}{d\epsilon}\frac{d\epsilon}{d\kappa} = Sr, \tag{6}$$

where Eqs.(4) and (5) are used. For the light with a wavelength of 1.55 μm, the strain coefficient S of a glass FBG is reported to be 1.2 pm/$\mu\varepsilon$ = 1.2×10^{-6} m [21]. The core pitch r of the MCF is 35.4 μm. Substituting these values into Eq.(6), we have $Sr = 42.5 \times 10^{-12}$ m^2, which supports the validity of the experimental results of 38.7×10^{-12} m^2 (MCFBG1), 43.3×10^{-12}m^2 (MCFBG2), and 45.9×10^{-12}m^2 (MCFBG3).

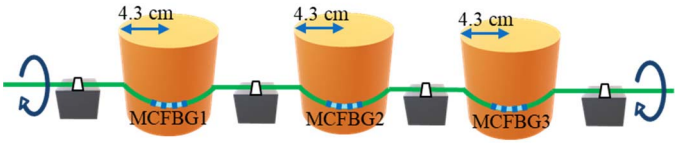

Fig. 9. Experimental setup of bending direction measurement. The sensing fiber is fixed on 4 cubes with MCBGs bent around the surface of the cylinders. The sensing fiber is rotated with the cubes every 90 degrees and the bending direction of MCFBGs is changed.

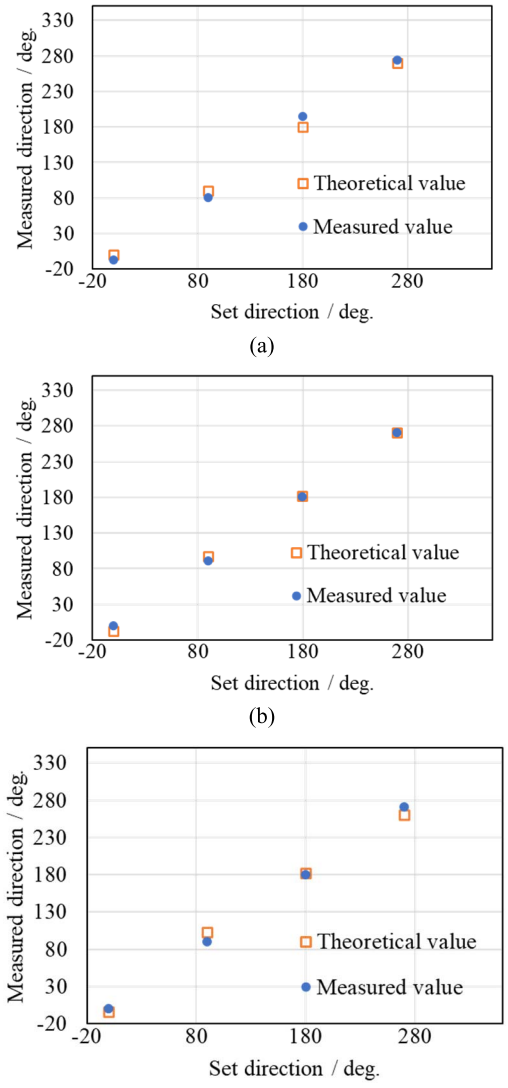

Fig. 10. Measurement results of bending in 4 directions for (a) MCFBG1, (b) MCFBG2, and (c) MCFBG3.

Next, the bending direction of the three MCFBG parts were changed every 90°. We attached the sensing fiber to four cubes and bent the three MCFBGs along three cylinders with a radius of 4.3 cm(Fig. 9). By rotating all the cubes in the

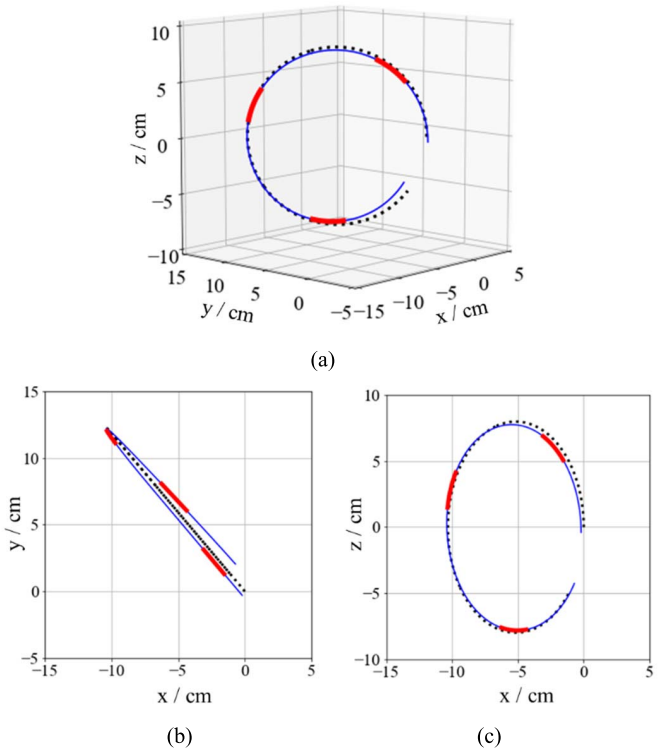

Fig. 11. Measured circle shape (a) in xyz space, (b) projected on xy plane, and (c) xz plane. The xyz coordinate is set just for viewability.

same direction at the same time, the surface of the MCFBG along the cylinder was rotated and the bending direction was changed. The bending directions were measured from the average value of five times measurements. Fig.10 shows that the measured direction agrees well with the set direction. The standard deviation is less than 2.02 °, which confirms the measurement accuracy.

C. Pilot Demonstration of Shape Measurement

We can measure the shape of the sensing fiber under the condition that there are not large changes of curvature along the sensing fiber. In this case, the bending shape of the entire fiber can be estimated from the measured curvature and bending direction of the MCFBG sections [22], [23]. We derived the bending shape on the assumption that the bending shape of the entire optical fiber was composed of multiple arcs. The radius of the arc was determined from the curvature of the MCFBG, and the central angle of the arc is determined by considering the distance between adjacent MCFBGs as the length of the arc. In our experiment, the arc length for one MCFBG was 0.15 m. We performed calculation so that the tangents of the neighboring two arcs coincide at the connecting part. Suppose that the effect of twisting is compensated, the direction of the two arcs is given by the bending direction of the MCFBGs.

As a proof-of-concept experiment, we wrapped the sensing fiber around a disk with a radius of 8.0 cm. The effect of twisting between the MCFBG parts was compensated by the data acquired in advance when the bending direction was constant. Fig.11 shows the experimental results (blue solid line) and the actual shape (dashed line). It can be confirmed that the overall bending shape derived from the bending shape of MCFBG (solid red line) is close to the actual bending shape. The root-mean-square error between the experimentally obtained shape and the actual one is 0.49 cm.

V. Conclusion

In this study, we have proposed and evaluated a multipoint bending sensing method for MCFBG using a simple system of intensity correlation measurement using TPA process in Si-APD. We have successfully discriminated the reflection spectra of 21 Bragg gratins even if they are overlapped in the wavelength region. The evaluation of proposed method has been performed by three-point measurement of curvature radius and direction, where the maximum error of wavelength shift was 0.0473 nm and that of direction was 2.02°. Furthermore, we have demonstrated the shape measurement of the sensing fiber with smoothly changing curvature. The proposed system does not require multiple detectors nor optical switching devices. Although our shape measurement was performed under the condition that the effect of fiber twisting was compensated beforehand, the use of a twisted multicore fiber would provide the information of twist and bending at the same time [24]. Our next plan is to apply our system to shape measurement of things such as medical catheters, robot arms, parts of buildings, and human body especially around chest area to measure the volume change due to breathing.

References

[1] M. S. Kovacevic, A. Djordjevich, and D. Nikezic, "Analytical optimization of optical fiber curvature gauges," *IEEE Sensors J.*, vol. 8, no. 3, pp. 227–232, Mar. 2008.
[2] Y. Fu, H. Di, and R. Liu, "Light intensity modulation fiber-optic sensor for curvature measurement," *Opt. Laser Technol.*, vol. 42, no. 4, pp. 594–599, 2010.
[3] D. Z. Stupar, J. S. Bajic, L. M. Manojlovic, M. P. Slankamenac, A. V. Joza, and M. B. Zivanov, "Wearable low-cost system for human joint movements monitoring based on fiber-optic curvature sensor," *IEEE Sensors J.*, vol. 12, no. 12, pp. 3424–3431, Dec. 2012.
[4] J. Ge, A. E. James, L. Xu, Y. Chen, K.-W. Kwok, and M. P. Fok, "Bidirectional soft silicone curvature sensor based on off-centered embedded fiber Bragg grating," *IEEE Photon. Technol. Lett.*, vol. 28, no. 20, pp. 2237–2240, Jul. 15, 2016.
[5] Y. Liu, J. A. R. Williams, and I. Bennion, "Optical bend sensor based on measurement of resonance mode splitting of long-period fiber grating," *IEEE Photon. Technol. Lett.*, vol. 12, no. 5, pp. 531–533, May 2000.
[6] T. Allsop *et al.*, "Bending characteristics of fiber long-period gratings with cladding index modified by femtosecond laser," *J. Lightw. Technol.*, vol. 24, no. 8, pp. 3147–3154, Aug. 1, 2006.
[7] A. Minardo, R. Bernini, and L. Zeni, "Bend-induced Brillouin frequency shift variation in a single-mode fiber," *IEEE Photon. Technol. Lett.*, vol. 25, no. 23, pp. 2362–2364, Oct. 10, 2013.
[8] Z. Zhao, M. A. Soto, M. Tang, and L. Thèvenaz, "Distributed shape sensing using Brillouin scattering in multi-core fibers," *Opt. Exp.*, vol. 24, no. 22, pp. 25211–25223, 2016.
[9] A. Issatayeva, A. Amantayeva, W. Blanc, D. Tosi, and C. Molardi, "Design and analysis of a fiber-optic sensing system for shape reconstruction of a minimally invasive surgical needle," *Sci. Rep.*, vol. 11, no. 1, pp. 1–12, 2021.
[10] G. Wei and Q. Jiang, "Needle shape sensing with Fabry–Pérot interferometers," *IEEE Sensors J.*, early access, Aug. 16, 2021, doi: 10.1109/JSEN.2021.3105383.
[11] E. Fujiwara, J. G. Hayashi, T. da Silva Delfino, P. A. S. Jorge, and C. M. de Barros Cordeiro, "Optical fiber anemometer based on a multi-FBG curvature sensor," *IEEE Sensors J.*, vol. 19, no. 19, pp. 8727–8732, Oct. 2019.

[12] E. Lindley *et al.*, "Demonstration of uniform multicore fiber Bragg gratings," *Opt. Exp.*, vol. 22, no. 25, pp. 31575–31581, 2014.
[13] G. M. H. Flockhart, W. N. MacPherson, J. S. Barton, J. D. C. Jones, L. Zhang, and I. Bennion, "Two-axis bend measurement with Bragg gratings in multicore optical fiber," *Opt. Lett.*, vol. 28, no. 6, p. 387, 2003.
[14] A. Donko, M. Beresna, Y. Jung, J. Hayes, D. J. Richardson, and G. Brambilla, "Point-by-point femtosecond laser micro-processing of independent core-specific fiber Bragg gratings in a multi-core fiber," *Opt. Exp.*, vol. 26, no. 2, p. 2039, 2018.
[15] D. Barrera, I. Gasulla, and S. Sales, "Multipoint two-dimensional curvature optical fiber sensor based on a nontwisted homogeneous four-core fiber," *J. Lightw. Technol.*, vol. 33, no. 12, pp. 2445–2450, Jun. 15, 2015.
[16] J. P. Moore and M. D. Rogge, "Shape sensing using multi-core fiber optic cable and parametric curve solutions," *Opt. Exp.*, vol. 20, no. 3, p. 2967, 2012.
[17] F. Khan, A. Denasi, D. Barrera, J. Madrigal, S. Sales, and S. Misra, "Multi-core optical fibers with Bragg gratings as shape sensor for flexible medical instruments," *IEEE Sensors J.*, vol. 19, no. 14, pp. 5878–5884, Jul. 2019.
[18] Y. Tanaka, M. Nemoto, and Y. Yamada, "Displacement measurement using two-photon absorption process in Si-avalanche photodiode and fiber Bragg gratings," *J. Lightw. Technol.*, vol. 36, no. 4, pp. 1192–1196, Feb. 15, 2018.
[19] Y. Tanaka and H. Miyasawa, "Multipoint fiber Bragg grating sensing using two-photon absorption process in silicon avalanche photodiode," *J. Lightw. Technol.*, vol. 36, no. 4, pp. 1032–1038, Feb. 15, 2018.
[20] Y. Tanaka, T. Abe, and H. Miyazawa, "Directional curvature sensing using multicore fiber Bragg grating and two-photon absorption process in Si-APD," in *Conf. Lasers Electro-Opt. (CLEO), OSA Tech. Dig. (Opt. Soc. Amer.)*, 2019, Paper SF3L.1.
[21] A. Kersey *et al.*, "Fiber grating sensors," *J. Lightw. Technol.*, vol. 15, no. 8, pp. 1442–1463, Aug. 1997.
[22] R. J. Roesthuis, M. Kemp, J. J. van den Dobbelsteen, and S. Misra, "Three-dimensional needle shape reconstruction using an array of fiber Bragg grating sensors," *IEEE/ASME Trans. Mechatronics*, vol. 19, no. 4, pp. 1115–1126, Aug. 2014.
[23] L. Xu, J. Ge, J. H. Patel, and M. P. Fok, "Dual-layer orthogonal fiber Bragg grating mesh based soft sensor for 3-dimensional shape sensing," *Opt. Exp.*, vol. 25, no. 20, p. 24727, 2017.
[24] P. S. Westbrook *et al.*, "Continuous multicore optical fiber grating arrays for distributed sensing applications," *J. Lightw. Technol.*, vol. 35, no. 6, pp. 1248–1252, Mar. 15, 2017.

Naohiro Sonoda received the B.E. degree in electrical and electronic engineering from Tokyo University of Agriculture and Technology (TUAT), Tokyo, Japan, in 2020. He is a Graduate Student with TUAT and working on fiber optic bending sensor using multicore fiber Bragg grating and two-photon absorption process in Si-APD.

Reina Takagi, photograph and biography not available at the time of publication.

Itsuki Saito, photograph and biography not available at the time of publication.

Tetsuya Abe, photograph and biography not available at the time of publication.

Shihua Zhao, photograph and biography not available at the time of publication.

Yosuke Tanaka (Member, IEEE) received the B.E. degree in electronic engineering and the M.E. and Dr. Eng. degrees in electrical engineering from the University of Tokyo, Tokyo, Japan, in 1991, 1993, and 1996, respectively. After working with Shizuoka University, as a Research Associate, he joined Tokyo University of Agriculture and Technology, Tokyo, in 1999, where he is currently an Associate Professor. His research interests include the fiber optic sensing and its related subjects, including laser-based precision measurement, highspeed optical signal processing, application of optical frequency comb, and fiber optic power supply. He is a member of OPTICA, the International Society for Optics and Photonics (SPIE), the Institute of Electronics, Information, and Communication Engineers (IEICE), and Japan Society of Applied Physics (JSAP).